



MINISTRY OF SUPPLY

AERONAUTICAL RESEARCH COUNCIL
REPORTS AND MEMORANDA

Some Actuator-Disc Theories for the Flow of Air Through an Axial Turbo-Machine

By

J. H. HORLOCK,

of the University of Cambridge, Department of Engineering

© *Crown Copyright* 1958

LONDON : HER MAJESTY'S STATIONERY OFFICE

1958

ELEVEN SHILLINGS NET

To estimate the magnitude of the differences between the various theories the direct problem of a single compressor stage has been considered, the stage consisting of one rotor and one stator.

The velocities at entry to the rotor and at exit from the stator are axial; the tangent of the outlet angle from the rotor varies linearly with radius and is equal to unity at the tip radius, *i.e.*, $\tan \beta = r/r_t = R$.

The hub-tip ratio is 0.4 and the 'aspect ratios' of the blades l/b are chosen as (i) 2.1, and (ii) 4.2, assuming negligible axial clearances. When the actuator discs are placed at the centres of pressure of the blades it is assumed that the distance of the centre of pressure from the blade trailing edge is two-thirds of the blade width, *i.e.*, ($a/b = 2/3$).

Such a stage is similar to an axial-flow-compressor test stage installed in the Cambridge University Engineering Laboratories. The tip diameter of this compressor is 14 in. and the rig is designed for 6,000 r.p.m. If a mean axial velocity of 200 ft/sec is assumed, the flow parameter $(U_t/C_{x1}) = 1.83$, where U_t = blade-tip speed; C_{x1} = axial velocity at upstream infinity and is assumed constant.

2. Approximate Methods of Calculating the Flow through an Axial Turbo-Compressor Machine.—The general methods developed using actuator-disc theory are used to calculate the flow through the model stage and are compared with Raily's theory, and with radial equilibrium solutions. The positions of the actuator planes are illustrated in Figs. 1 and 2 for each method.

Method 1.—Radial Equilibrium Conditions at the Trailing Edges of the Blade Rows

For this theory conditions at stations (02), (2e) and (2) become identical, as do stations (04), (4e) and (4).

The radial equilibrium condition at the trailing edge of a rotor is then expressed by:

$$C_{x2} \frac{dC_{x2}}{dr} + \frac{1}{r^2} (rC_{u2}) \frac{d}{dr} (rC_{u2}) = \frac{dH_2}{dr}, \quad \dots \dots \dots \quad (2)$$

where

$$C_{u2} = U - C_{x2} \tan \beta_2$$

and

$$H_2 = H_1 + U(C_{u2} - C_{u1}).$$

For the particular example of the model stage, $\tan \beta_2 = r/r_t = R$,

and

$$\frac{dH_2}{dr} = \frac{d}{dr} \{U(U - C_{x2} \tan \beta_2)\}.$$

Then equation (2) reduces to:

$$\frac{dC_{x2}}{dR} + C_{x2} \left(\frac{2R}{1 + R^2} \right) = \frac{2U_t R}{(1 + R^2)},$$

which gives an exact solution:

$$\frac{C_{x2}}{C_{x1}} = \frac{P_1 + \frac{U_t}{C_{x1}} R^2}{(1 + R^2)} \quad \dots \dots \dots \quad (3)$$

where P_1 is a constant to be determined from the continuity conditions:

$$\int_{R_h}^1 C_{x2} R dR = \int_{R_h}^1 C_{x1} R dR$$

and is given thus:

$$P_1 = \frac{\left(1 - \frac{U_t}{C_{x1}}\right) (1 - R_h^2) + \frac{U_t}{C_{x1}} \log_e \left(\frac{2}{1 + R_h^2}\right)}{\log_e \left(\frac{2}{1 + R_h^2}\right)}$$

Similarly at the trailing edge of the following stator:

$$C_{x4} \frac{dC_{x4}}{dr} + \frac{1}{r^2}(rC_{u4}) \frac{d}{dr}(rC_{u4}) = \frac{dH_4}{dr} \quad \dots \quad \dots \quad \dots \quad \dots \quad \dots \quad (4)$$

where $C_{u4} = C_{x4} \tan \alpha_4$.

For the particular example, $\tan \alpha_4 = 0$,

so that:

$$\begin{aligned} C_{x4} \frac{dC_{x4}}{dr} &= \frac{dH_4}{dr} \\ &= \frac{d}{dr}\{U(U - C_{x2} \tan \beta_2)\}, \end{aligned}$$

whence it may be shown:

$$\frac{C_{x4}}{C_{x1}} = \left\{ 2 \left(\frac{U_t}{C_{x1}} \right) \left(\frac{U_t}{C_{x1}} - P_1 \right) \frac{R^2}{1 + R^2} + Q_1 \right\}^{1/2}, \quad \dots \quad \dots \quad \dots \quad (5)$$

where Q_1 is a constant and is determined by trial and error from the continuity relation.

It is of interest to note that if the outlet air angles β_2 and α_4 are assumed constant with incidence, then the off-design conditions are easily obtained by using a different value of U_t/C_{x1} .

Actuator-Disc General Theory.

By using the result that the axial velocity at an actuator disc stationed at the plane $x = 0$ is approximately $(C_{x1} + C_{x2})/2$, where C_{x1} and C_{x2} are the axial velocities at upstream and downstream infinity ($x = -\infty, +\infty$) and also assuming that the radial velocity at any point (r, x) is given by:

$$C_r = \sum_{i=1}^{i=\infty} \{ \exp(k_i x) \} f_i(r), \quad \dots \quad \dots \quad \dots \quad \dots \quad \dots \quad (1)$$

it may be shown that the axial velocity is given approximately by:

$$\left. \begin{aligned} C_x &= C_{x2} - \frac{(C_{x2} - C_{x1})}{2} \exp\{-(kx/l)\} & x > 0 \\ C_x &= C_{x1} + \frac{(C_{x2} - C_{x1})}{2} \exp\{(kx/l)\} & x < 0 \end{aligned} \right\}, \quad \dots \quad \dots \quad (6)$$

where l is the blade height and k is determined uniquely by the hub-tip ratio of the actuator disc.

This theory is developed in Ref. 5, and is given in Appendix I.

Further, the effect of neighbouring blade rows is obtained by superimposing the vortex sheets due to each disc, and then subtracting the vortex sheets at infinity. (The analysis is based upon the values of k obtained from the isolated actuator-disc theory and the justification for this approximation is investigated in the calculations for the model stage.)

If the actuator discs are placed at the trailing edges of the blade rows the axial velocity at the p th disc C_{x0p} is then given by:

$$\begin{aligned} C_{x0p} &= \frac{C_{xp+1} + C_{xp}}{2} - \sum_{q=1}^{q=p-1} \left(\frac{C_{xq+1} - C_{xq}}{2} \right) \{ \exp - (k_q x_{pq}/l_q) \} \\ &\quad + \sum_{q=p+1}^{q=n} \left(\frac{C_{xq+1} - C_{xq}}{2} \right) \{ \exp - (k_q x_{pq}/l_q) \} \quad \dots \quad \dots \quad (7) \end{aligned}$$

where $C_{x_p}, C_{x_{p+1}}$ are the axial velocities that would exist at upstream and downstream infinity of the p th row if that row were isolated, due to the discontinuities in tangential velocity and vorticity at that row.

$C_{x_q}, C_{x_{q+1}}$ are similarly defined and x_{pq} is the distance (always positive) between the p th and q th rows.

(Equation (7) is also obtained in Ref. 5 as in Appendix I.)

If, however, the actuator discs are placed at the blade centres of pressure then the axial velocity at the p th trailing edge $C_{x_{pe}}$ is given by:

$$C_{x_{pe}} = C_{x_{p+1}} - \sum_{q=1}^{q=p} \frac{(C_{x_{q+1}} - C_{x_q})}{2} \{ \exp - (k_q x_{peq} / l_q) \} + \sum_{q=p+1}^{q=n} \left(\frac{C_{x_{q+1}} - C_{x_q}}{2} \right) \{ \exp - (k_q x_{peq} / l_q) \}, \quad \dots \quad (8)$$

where x_{peq} is the distance between the p th trailing edge and the q th disc.

Marble has given a solution of the inverse problem in which the distribution of tangential velocity is initially specified, but the direct problem (that of determining the flow conditions if the air angles are specified) results in a series of functional equations, since the change in whirl velocity at the p th row is itself dependent upon $C_{x_{0p}}$. Methods of successive approximation to solve this problem are given below in Methods 3 and 4.

Method 2.—Isolated Actuator Discs placed at the Trailing Edges of the Blades

If the rows are sufficiently far apart the effects of blade interference may be neglected and the following analysis is developed.

Bragg and Hawthorne³ have given a general equation for the incompressible, axially symmetric flow on either side of an actuator disc:

$$\frac{dH}{d\psi} = \frac{1}{r^2} \left[\Theta \frac{d\Theta}{d\psi} + \eta r \right] \dots \dots \dots (9)$$

Across an actuator disc:

$$H_{02} = H_{01} + \Delta W, \quad \dots \dots \dots (10)$$

where ΔW is the work done on the fluid by the moving blade row and is given by:

$$\Delta W = U(C_{u_{02}} - C_{u_{01}}) \dots \dots \dots (11)$$

From equations (9), (10), (11):

$$\left\{ \eta_{02} r + r C_{u_{02}} \frac{d}{d\psi} (r C_{u_{02}}) \right\} = \left\{ \eta_{01} r + r C_{u_{01}} \frac{d}{d\psi} (r C_{u_{01}}) \right\} + r^2 \frac{d}{d\psi} \{ U(C_{u_{02}} - C_{u_{01}}) \},$$

which may be written:

$$\eta_{02} + (C_{u_{02}} - U) \frac{d}{d\psi} (r C_{u_{02}}) = \eta_{01} + (C_{u_{01}} - U) \frac{d}{d\psi} (r C_{u_{01}}) \dots \dots \dots (12)$$

But Bragg and Hawthorne have shown that Θ, H are functions of ψ , and for small streamline displacements, will be approximately constant at a given radius on either side of the disc. Further, Ruden's assumption (Appendix I) may be made, that the tangential vorticity is approximately a function of radius alone.

Thus

$$\eta_{01} \simeq \eta_1 = \left(\frac{\partial C_r}{\partial x} \right)_1 - \left(\frac{\partial C_x}{\partial r} \right)_1 = - \frac{dC_{x1}}{dr} \left. \dots \dots \dots \right. (13)$$

$$\eta_{02} \simeq \eta_2 = \left(\frac{\partial C_r}{\partial x} \right)_2 - \left(\frac{\partial C_x}{\partial r} \right)_2 = - \frac{dC_{x2}}{dr}$$

Further $C_{u01} = C_{x01} \tan \alpha_{01} = C_{x1} \tan \alpha_1$,
 and if the disc is placed at the trailing edge of the blades: $C_{u02} = U - C_{x02} \tan \beta_{02} = C_{x2} \tan \alpha_2$ } (14)

Hence equation (12) becomes:

$$\begin{aligned} \frac{dC_{x2}}{dr} + C_{x02} \tan \beta_{02} \frac{d}{d\psi} \{r(U - C_{x02} \tan \beta_{02})\} \\ = \frac{dC_{x1}}{dr} + (U - C_{x1} \tan \alpha_1) \frac{d}{d\psi} \{rC_{x1} \tan \alpha_1\}. \end{aligned}$$

But $C_{x01} = C_{x02} = \frac{C_{x1} + C_{x2}}{2}$ (Ref. 8), and the further approximation is made that:

$$rC_{x02} \approx -\frac{d\psi}{dr},$$

i.e., $\frac{d}{d\psi} = -\frac{1}{rC_{x02}} \frac{d}{dr}$,

so that:

$$\begin{aligned} \frac{dC_{x2}}{dr} - \frac{\tan \beta_{02}}{r} \frac{d}{dr} \left[r \left\{ U - \left(\frac{C_{x1} + C_{x2}}{2} \right) \tan \beta_{02} \right\} \right] \\ = \frac{dC_{x1}}{dr} - \frac{2(U - C_{x1} \tan \alpha_1)}{r(C_{x1} + C_{x2})} \frac{d}{dr} (rC_{x1} \tan \alpha_1). \end{aligned} \quad \dots \quad (15)$$

This may be written as an equation of the form:

$$C_{x2}^2 + A_2(r)C_{x2} \frac{dC_{x2}}{dr} + B_2(r)C_{x2} + C_2(r) \frac{dC_{x2}}{dr} + D_2(r) = 0. \quad \dots \quad (15a)$$

A similar analysis for a disc representing a stator ($\Delta H = 0$) gives:

$$\begin{aligned} \frac{dC_{x4}}{dr} + \frac{\tan \alpha_{04}}{r} \frac{d}{dr} \left\{ r \frac{(C_{x3} + C_{x4})}{2} \tan \alpha_{04} \right\} \\ = \frac{dC_{x3}}{dr} + \frac{2C_{x3}}{(C_{x3} + C_{x4})} \frac{\tan \alpha_3}{r} \frac{d}{dr} (rC_{x3} \tan \alpha_3), \end{aligned} \quad \dots \quad (16)$$

which reduces to a similar differential equation in C_{x4} :

$$C_{x4}^2 + A_4(r)C_{x4} \frac{dC_{x4}}{dr} + B_4(r)C_{x4} + C_4(r) \frac{dC_{x4}}{dr} + D_4(r) = 0. \quad \dots \quad (16a)$$

Equations (15) and (16) are general for any actuator discs placed at the blade trailing edges and operating at planes sufficiently far from other discs that the effect of blade interference is negligible. Thus the velocity profiles through a turbo-machine may be obtained row by row by assuming the axial velocity upstream of a row is given by that at downstream infinity in the solution to the preceding disc, and the whirl velocity upstream is specified by the conditions immediately downstream of the preceding disc.

Thus $A(r)$, $B(r)$, $C(r)$ and $D(r)$ are all known for the direct problem and equations similar to (15) and (16) may be found. These are usually non-linear differential equations but are easily solved graphically, by successive approximation and integration. It is of interest to note that equations (15) and (16) take into account a variation in inlet total head and axial velocity.

For the model stage accepting a uniform upstream profile equation (15) reduces to:

$$\frac{dC_{x2}}{dR} \left(1 + \frac{R^2}{2}\right) + C_{x2}R = (2U_t - C_{x1})R,$$

which gives an exact solution:

$$\frac{C_{x2}}{C_{x1}} = \frac{P_2 + \left(\frac{2U_t}{C_{x1}} - 1\right) R^2}{(2 + R^2)}, \dots \dots \dots (17)$$

where

$$P_2 = \frac{2\left(1 - \frac{U_t}{C_{x1}}\right) (1 - R^2)}{\log_e \left(\frac{3}{2 + R^2}\right)} - 2\left(1 - \frac{2U_t}{C_{x1}}\right)$$

from the continuity relation. The equation for the following stator reduces to:

$$\frac{dC_{x4}}{dR} = \frac{dC_{x3}}{dR} + \frac{2C_{x3}}{C_{x3} + C_{x4}} \tan \alpha_3 \frac{d}{dR} (RC_{x3} \tan \alpha_3) \dots \dots \dots (18)$$

But

$$C_{x3} \tan \alpha_3 = \left(U - \frac{C_{x1} + C_{x2}}{2} \tan \beta_{02}\right)$$

where $\tan \beta_{02} = R$ and $C_{x2} = C_{x3}$ is obtained from equation (17).

The resulting equation is solved graphically.

Method 3.—Isolated Actuator Discs placed at the Centres of Pressure of the Blades

By equating $dH/d\psi$ on each side of an actuator disc placed at the blade centres of pressure, equation (12) is obtained as before. However, the whirl velocity C_{u02} is no longer specified by the axial velocity at the disc, but by the conditions at the trailing edge.

The whirl velocity is approximately constant downstream of the disc since $\theta = rC_u$ is constant along a streamline and radial displacements are small.

Thus
$$\left. \begin{aligned} C_{u02} &= C_{u2e} \\ \text{and } C_{u2e} &= U - C_{x2e} \tan \beta_{2e} \end{aligned} \right\}, \dots \dots \dots (19)$$

where C_{x2e} is obtained from equation (6).

$$C_{x2e} = C_{x2} - \frac{(C_{x2} - C_{x1})}{2} \{\exp(-ka/l)\} = C_{x2} \left(1 - \frac{K_a}{2}\right) + C_{x1} \left(\frac{K_a}{2}\right), \dots \dots (20)$$

where a is the axial distance between the planes of the centre of pressure and the trailing edge, and $K_a = \{\exp(-ka/l)\}$.

Thus

$$\begin{aligned} \frac{dC_{x2}}{dr} + C_{x2e} \tan \beta_{2e} \frac{d}{d\psi} \{r(U - C_{x2e} \tan \beta_{2e})\} \\ = \frac{dC_{x1}}{dr} + (U - C_{x1} \tan \alpha_1) \frac{d}{d\psi} (rC_{x1} \tan \alpha_1). \end{aligned}$$

This differential equation may be integrated graphically to give a relation between (C_{x4}/C_{x1}) and (C_{x2}/C_{x1}) , which together with equations (25) and (26) enables (C_{x2}/C_{x1}) to be calculated. With (C_{x2}/C_{x1}) and (C_{x4}/C_{x1}) known, (C_{x02}/C_{x1}) and (C_{x04}/C_{x1}) are directly obtained from equation (25). This has been done for two examples in which $l/b = 2.1$ and 4.2 .

Method 5.—Actuator Discs placed at the Centres of Pressures of the Blades—Blade-Interference Theory

If the actuator discs are placed at the centres of pressure of the blades as Marble suggests, then the whirl velocities are defined not by the axial velocities at the discs themselves but by the axial velocities at the trailing-edge positions $(C_{x1e}, C_{x2e} \dots C_{xpe}, C_{xqe} \dots C_{xne})$ downstream of the discs.

These whirl velocities are:

$$\left. \begin{array}{l} \text{for the } p\text{th row, if a rotor } C_{u\,pe} = U - C_{x\,pe} \tan \beta_{pe} \\ \text{for the } p\text{th row, if a stator } C_{u\,pe} = C_{x\,pe} \tan \alpha_{pe} \end{array} \right\}, \quad \dots \quad (29)$$

where β_{pe}, α_{pe} are the rotor and stator exit air angles at the trailing edges, measured relative to the blade rows.

Since the value of $\theta = rC_u$ is constant along a streamline between the discs, for small streamline displacements the whirl velocity C_u is constant.

Thus the whirl velocity C_u just downstream of an actuator disc is defined by the axial velocity at the following trailing edge.

The method of solution of the problem is similar to that of Method 4. The 'downstream infinity' values of axial velocity are guessed and the velocities at the trailing-edge stations are calculated using the principle of superimposing the individual trailing vortex sheets due to each blade row, and subtracting those extending from upstream to downstream infinity.

For the trailing edge downstream of the p th row the axial velocity $C_{x\,pe}$ at that station is given by:

$$C_{x\,pe} = C_{x\,p+1} + \sum_{q=1}^{q=p} \left(\frac{C_{x\,q+1} - C_{x\,q}}{2} \right) \{ \exp(-k_q x_{pe\,q}/l_q) \} - \sum_{q=p+1}^{q=n} \left(\frac{C_{x\,q+1} - C_{x\,q}}{2} \right) \{ \exp(-k_q x_{pe\,q}/l_q) \}, \quad \dots \quad (8)$$

where $x_{pe\,q}$ is the distance (always positive) between the q th row and the p th trailing edge and the flow is incompressible.

For each disc a differential equation is obtained similar to equations (15) or (16) but the whirl velocities just downstream of the disc are the same as those calculated for the trailing edge:

for the p th row a rotor $C_{0p} = C_{u\,pe} = U - C_{x\,pe} \tan \beta_{pe}$

for the p th row a stator $C_{u\,0p} = C_{u\,pe} = C_{x\,pe} \tan \alpha_{pe}$.

Thus for the p th row if a rotor:

$$\begin{aligned} \frac{dC_{x\,p+1}}{dr} - \frac{2C_{x\,pe} \tan \beta_{pe}}{r(C_{x\,p+1} + C_{x\,p})} \frac{d}{dr} \{ r(U - C_{x\,pe} \tan \beta_{pe}) \} \\ = \frac{dC_{x\,p}}{dr} - \frac{2(U - C_{x\,(p-1)e} \tan \alpha_{(p-1)e})}{r(C_{x\,p+1} + C_{x\,p})} \frac{d}{dr} \{ r C_{x\,(p-1)e} \tan \alpha_{(p-1)e} \}, \quad \dots \quad (30) \end{aligned}$$

or for a stator:

$$\begin{aligned} \frac{dC_{x\,p+1}}{dr} + \frac{2C_{x\,pe} \tan \alpha_{pe}}{r(C_{x\,p+1} + C_{x\,p})} \frac{d}{dr} \{ r(C_{x\,pe} \tan \alpha_{pe}) \} \\ = \frac{dC_{x\,p}}{dr} + \frac{2(U - C_{x\,(p-1)e} \tan \beta_{(p-1)e})}{r(C_{x\,p+1} + C_{x\,p})} \frac{d}{dr} \{ r(U - C_{x\,(p-1)e} \tan \beta_{(p-1)e}) \}, \quad \dots \quad (31) \end{aligned}$$

The n equations for the n blade rows are then simply solved by graphical integration and the resulting values of 'downstream infinity' axial velocities may be used in a second approximation. For the model stage:

$$\text{and } \left. \begin{aligned} C_{x_{2e}} &= C_{x_2} + \frac{K_{b-a}(C_{x_4} - C_{x_2})}{2} - \frac{K_a(C_{x_2} - C_{x_1})}{2} \\ C_{x_{4e}} &= C_{x_4} - \frac{K_{a+b}(C_{x_2} - C_{x_1})}{2} - \frac{K_a(C_{x_4} - C_{x_2})}{2} \end{aligned} \right\} \dots \dots \dots (32)$$

where $K_{b-a} = \exp \{[-k(b-a)]/l\}$, $K_a = \exp(-ka/l)$, $K_{a+b} = \exp \{[-k(a+b)]/l\}$, in which b is the axial distance between the discs (*i.e.*, the blade-row centres of pressure), and a is the axial distance between the actuator-disc stations and the trailing edges of the blades.

Then as in Method 4:

$$\text{But } \frac{dC_{x_4}}{dr} = \frac{dC_{x_2}}{dr} \left\{ 1 + \frac{(U - C_{x_{2e}} \tan \beta_{2e})(C_{x_1} + C_{x_2})}{(C_{x_2} + C_{x_4})(C_{x_{2e}} \tan \beta_{2e})} \right\}$$

$$C_{x_{2e}} = C_{x_2} \left(1 - \frac{K_a + K_{b-a}}{2} \right) + \frac{K_{b-a}}{2} C_{x_4} + \frac{K_a}{2} C_{x_1}$$

$$\frac{d \left(\frac{C_{x_4}}{C_{x_1}} \right)}{d \left(\frac{C_{x_2}}{C_{x_1}} \right)} = \frac{\left(2 \frac{U}{C_{x_1}} - K_a \right) + (K_a + K_{b-a}) \frac{C_{x_2}}{C_{x_1}} + (1 - K_{b-a}) \frac{C_{x_4}}{C_{x_1}}}{\left(\frac{C_{x_2} + C_{x_4}}{C_{x_1}} \right)}, \dots \dots \dots (33)$$

whence the method of solution is the same as before.

Ultimate Steady Flow.—Stages deeply embedded in an axial-flow turbo-machine may be considered as identical pairs of actuator discs and the distribution of the tangential vorticity η_R is the same after each rotor row. C_{x_R} is defined as that axial velocity that would exist far downstream of the rotor and is related to η_R by $\eta_R = -(dC_{x_R}/dr)$. Similarly the distribution of tangential vorticity $\eta_S = -(dC_{x_S}/dr)$ is the same after each identical stator.

If the rotor, say the k th row is considered then along a streamline:

$$H_k = H_{k-1} + \Delta W_k, \dots \dots \dots (34)$$

where H_{k-1} is the stagnation enthalpy after the $(k-1)$ th disc

H_k is the stagnation enthalpy after the k th disc

ΔW_k is the work done on the fluid by the k th row.

For the $(k+1)$ th row, a stator row:

$$\begin{aligned} \Delta W_{k+1} &= 0, \\ H_k &= H_{k+1}. \dots \dots \dots (35) \end{aligned}$$

Then from equations (34) and (35), along a given streamline $H_{k+1} = H_{k-1} + \Delta W_k$.

Differentiating with respect to ψ ,

$$\left(\frac{dH_{k+1}}{d\psi} \right) = \left(\frac{dH_{k-1}}{d\psi} \right) + \frac{d}{d\psi} (\Delta W_k),$$

but using equation (9) for the $(k - 1)$ th row, a stator:

$$\left(\frac{dH_{k-1}}{d\psi}\right) = \frac{1}{r^2} \left(\eta_s r + \theta_s \frac{d\theta_s}{d\psi}\right) = \left(\frac{dH_{k+1}}{d\psi}\right)$$

for small streamline displacements. Hence $d(\Delta W_k)/dr = 0$. Or approximately:

$$\frac{d}{d\psi} (\Delta W_k) = 0, \quad \dots \dots \dots \dots \dots \dots \dots \dots \dots \dots \quad (36)$$

result originally given by A. R. Howell⁷ and used by Raily⁸.

Method 6.—Actuator Discs placed at the Trailing Edges of the Blades—Ultimate Steady Flow

If the actuator discs are placed at the trailing edges of the blades then:

$$\frac{d}{dr} [U\{(U - C_{x0R} \tan \beta_{0R}) - C_{x0S} \tan \alpha_{0S}\}] = 0 \dots \dots \dots \dots \quad (36a)$$

Then if an infinite number of identical rows is considered, using equation (12) the axial velocity at any rotor disc C_{x0R} is given by:

$$\begin{aligned} C_{x0R} &= \left(\frac{C_{xR} + C_{xS}}{2}\right) - \left(\frac{C_{xR} - C_{xS}}{2}\right) \left\{ \left(\exp - \frac{2kb}{l}\right) + \left(\exp - \frac{4kb}{l} \dots\right) \right\} \\ &\quad - \left(\frac{C_{xS} - C_{xR}}{2}\right) \left\{ \left(\exp - \frac{kb}{l}\right) + \left(\exp - \frac{3kb}{l} \dots\right) \right\} \\ &\quad + \left(\frac{C_{xR} - C_{xS}}{2}\right) \left\{ \left(\exp - \frac{2kb}{l}\right) + \left(\exp - \frac{4kb}{l} \dots\right) \right\} \\ &\quad + \left(\frac{C_{xS} - C_{xR}}{2}\right) \left\{ \left(\exp - \frac{kb}{l}\right) + \left(\exp - \frac{3kb}{l} \dots\right) \right\} \\ &= \frac{C_{xR} + C_{xS}}{2} \\ &= C_{x0S} \dots \dots \dots \dots \dots \dots \dots \dots \dots \dots \quad (37) \end{aligned}$$

Thus equation (36a) becomes:

$$\frac{d}{dr} [U\{U - C_{x0R}(\tan \beta_{0R} + \tan \alpha_{0S})\}] = 0,$$

the result derived by Raily by superimposition of radial velocity fields.

Thus for the model stage in ultimate steady flow:

$$\frac{d}{dr} (\Delta W_k) = \frac{d}{dR} \{U(U - C_{x0R}R)\} = 0,$$

whence $C_{x0R} = \Omega + (\text{Constant}/R^2)$.

From the continuity relation the constant is determined and for the particular example ($U_i/C_{x1} = 1.83$):

$$\frac{C_{x0R}}{C_{x1}} = \frac{C_{x0S}}{C_{x1}} = 1.83 - \frac{0.381}{R^2} \dots \dots \dots \dots \dots \dots \dots \quad (38)$$

Method 7.—Actuator Discs placed at the Centres of Pressure of the Blades—Ultimate Steady Flow

If the actuator discs are placed at the centres of pressure of the blades then the equation (37) remains unchanged and $C_{x0R} = C_{x0S}$, although in general the values of C_{xR} and C_{xS} will be different from those used in Method 6.

However, the axial velocity at the trailing edge of any rotor is not the same as that at the trailing edge of a stator. For if the blade spacing is b , and the distance between the plane of the centre of pressure and the trailing edge is a , then for identical blade rows:

$$\begin{aligned}
 C_{xRe} = C_{xR} - \frac{(C_{xS} - C_{xR})}{2} & \left[\exp \left\{ -\frac{k}{l} (b + a) \right\} + \exp \left\{ -\frac{k}{l} (3b + a) \right\} + \dots \right] \\
 & - \frac{(C_{xR} - C_{xS})}{2} \left[\exp \left\{ -\frac{k}{l} a \right\} + \exp \left\{ -\frac{k}{l} (2b + a) \right\} + \dots \right] \\
 & + \frac{(C_{xS} - C_{xR})}{2} \left[\exp \left\{ -\frac{k}{l} (b - a) \right\} + \exp \left\{ -\frac{k}{l} (3b - a) \right\} + \dots \right] \\
 & + \frac{(C_{xR} - C_{xS})}{2} \left[\exp \left\{ -\frac{k}{l} (2b - a) \right\} + \exp \left\{ -\frac{k}{l} (4b - a) \right\} + \dots \right], \quad \dots \quad (39)
 \end{aligned}$$

$$\begin{aligned}
 C_{xSe} = C_{xS} - \frac{(C_{xR} - C_{xS})}{2} & \left[\exp \left\{ -\frac{k}{l} (b + a) \right\} + \exp \left\{ -\frac{k}{l} (3b + a) \right\} + \dots \right] \\
 & - \frac{(C_{xS} - C_{xR})}{2} \left[\exp \left\{ -\frac{k}{l} a \right\} + \exp \left\{ -\frac{k}{l} (2b + a) \right\} + \dots \right] \\
 & + \frac{(C_{xR} - C_{xS})}{2} \left[\exp \left\{ -\frac{k}{l} (b - a) \right\} + \exp \left\{ -\frac{k}{l} (3b - a) \right\} + \dots \right] \\
 & + \frac{(C_{xS} - C_{xR})}{2} \left[\exp \left\{ -\frac{k}{l} (2b - a) \right\} + \exp \left\{ -\frac{k}{l} (4b - a) \right\} + \dots \right] \quad \dots \quad (40)
 \end{aligned}$$

$$C_{xRe} \neq C_{xSe}.$$

The criterion $d(\Delta W_k)/dr = 0$ is still valid but the work done across a disc is defined by the whirl velocities at the trailing edge positions,

$$i.e., \quad \frac{d}{dr} [U\{(U - C_{xRe} \tan \beta_{Re}) - C_{xSe} \tan \alpha_{Se}\}] = 0. \quad \dots \quad (36b)$$

This equation is not sufficient to determine the flow as in Method 6 since $C_{xRe} \neq C_{xSe}$, and a method of successive approximation must be used. C_{xR} and C_{xS} may be guessed and two differential equations are integrated graphically.

Thus for a rotor:

$$\begin{aligned}
 \frac{dC_{xR}}{dr} - \frac{2C_{xRe} \tan \beta_{Re}}{r(C_{xR} + C_{xS})} \frac{d}{dr} \{r(U - C_{xRe} \tan \beta_{Re})\} \\
 = \frac{dC_{xS}}{dr} - \frac{2(U - C_{xSe} \tan \alpha_{Se})}{r(C_{xR} + C_{xS})} \frac{d}{dr} (rC_{xSe} \tan \alpha_{Se}). \quad \dots \quad (41)
 \end{aligned}$$

And for any stator:

$$\begin{aligned}
 \frac{dC_{xS}}{dr} + \frac{2C_{xSe} \tan \alpha_{Se}}{r(C_{xR} + C_{xS})} \frac{d}{dr} (rC_{xSe} \tan \alpha_{Se}) \\
 = \frac{dC_{xR}}{dr} + \frac{2(U - C_{xRe} \tan \beta_{Re})}{r(C_{xR} + C_{xS})} \frac{d}{dr} \{r(U - C_{xRe} \tan \beta_{Re})\} \dots \dots \quad (42)
 \end{aligned}$$

These two equations together with the values of C_{xRe} , C_{xSe} obtained from equations (39) and (40) and the guessed values of C_{xR} , C_{xS} enable a solution to be obtained, or alternatively either equation (41) or equation (42) may be used together with (36b).

It is of interest to note that for the model stage the criterion $d(\Delta W_k/dr) = 0$ gives the distribution of C_{xRe} with radius immediately since $\tan \alpha_{Se} = 0$, and this gives C_{xRe} as identical to $C_{x0R} = C_{x0S}$ calculated in Method 6. Then referring to equation (41):

$$\frac{dC_{xR}}{dr} = \frac{dC_{xS}}{dr},$$

since $\tan \alpha_{Se} = 0$ and $\frac{d}{dr}(\Delta W_k) = \Omega \frac{d}{dr} \{r(U - C_{xRe} \tan \beta_{Re})\} = 0$.

Hence $C_{xR} = C_{xS} + \text{constant}$.

The continuity relation requires that this constant should be zero so that $C_{xR} = C_{xS} = C_{x0R} = C_{x0S} = C_{xRe} = C_{xSe}$, i.e., there are no discontinuities in tangential vorticity across the discs.

Method 8.—Actuator-Disc Theory—Addition of Radial Fields (Railly)

Calculations for the model stage receiving a uniform upstream profile alone using the theory of addition of radial velocity fields have been made for comparison with Methods 2, 4 and 6 ($l/b = 2.1, 4.2$).

Values of K_b calculated from Railly's analysis are:

(a) $\frac{l}{b} = 2.1 \quad K_{b1} = 0.191 \quad K_{b2} = 0.192 \quad \text{cf. } K_b = 0.214$
from the isolated-disc theory

(b) $\frac{l}{b} = 4.2 \quad K_{b1} = 0.436 \quad K_{b2} = 0.446 \quad \text{cf. } 0.462$.

The addition of radial velocity fields gives the same result as Methods 6 and 7, for the model stage in ultimate steady flow. Methods 6 and 8 would give identical results for any given distribution of outlet air angles, β_R and α_S , in ultimate steady flow, but Method 7 in general gives different values for C_{xRe} , C_{xSe} .

Off-design Performance.—The exact solutions for Methods 1 and 2 have been used to compute the axial velocity at exit from the model stage rotor for $U_i/C_{x1} = 3.0$ assuming that the outlet angles α_2 remain unaltered.

3. Discussion of Calculations.—The calculation of axial velocity at rotor and stator trailing edges for the eight methods used are shown in Figs. 4 to 18.

The flow parameter U_i/C_{x1} has been chosen as 1.83, and for the methods involving the estimation of blade interference values of $l/b = 2.1, 4.2$ and $a/b = 2/3$ have been used.

In general the radial equilibrium solution (Method 1) has been used as a reference velocity.

In the discussion the effects of blade interference, positive interference from another disc is defined as that causing the axial velocity at the station considered to become more distorted from the value $C_x/C_{x1} = 1.0$. Negative interference implies that an external blade row is inducing a return to the undisturbed upstream velocity distribution. Thus it will be apparent that for the model stage the effect of the stator upon the rotor is a positive interference effect, but negative interference is induced at the stator disc by the rotor.

Figs. 4 to 6 compare the radial equilibrium approximation (Method 1) with a calculation for isolated actuator discs at the blade trailing edges (Method 2). There is a considerable difference in the computed axial velocities at the rotor trailing edges and at the stator-blade root.

Figs. 7 to 9 show the results obtained if the actuator disc is placed at the centre of pressure of the blade (Method 3). For the low aspect ratio blade ($l/b = 2.1$ $a/b = 2/3$), Fig. 7 shows this calculation to be near the radial equilibrium solution but the ratio $l/b = 4.2$ gives an axial velocity $C_{x_{2e}}$ little different from Method 2.

Figs. 8 and 9 suggest only small differences between the calculations for the stator. The calculations for $l/b = 2.1$ are almost identical with those for $l/b = 4.2$ and are not plotted.

Comparisons between Methods 4 and 8 and for blade interference have been made and excellent agreement is obtained. This is illustrated in Fig. 10. The rotor trailing-edge velocity is identical for $l/b = 2.1$, and the differences for $l/b = 4.2$ are small. Similar calculations for $C_{x_{04}}/C_{x_1}$ and C_{x_4}/C_{x_1} give close agreement, and the determination of the attenuation constant k_1 shows but small differences (see above).

The general effects of blade interference are therefore shown using the methods employing the concept of constancy of trailing vorticity (Hawthorne. Ref. 5. Appendix B).

Fig. 11 illustrates the small positive interference effect of the stator upon the rotor for $l/b = 2.1$ and a larger induced distortion from $C_{x_4}/C_{x_1} = 1$ for $l/b = 4.2$. Method 4, in which the discs are placed at the trailing edge, is employed.

Negative interference is shown by this method in Fig. 12, but Fig. 13 again suggests that the calculation of C_{x_4} varies little with the method chosen.

Figs. 14 to 16 illustrate Method 5, using blade-interference theory with the discs placed at the blade centres of pressure.

For the axial velocity at the rotor trailing edge, the separate effects of (i) placing the disc at the trailing edge (Fig. 7) and (ii) positive interference from the stator (Fig. 11) are combined (Fig. 14) and the result is little different from the radial equilibrium result. The calculations for $l/b = 2.1$ are not shown, as these are almost identical with the Method 1 results.

However, if the radial equilibrium calculation is fortuitously accurate for the rotor because of positive interference, negative interference at the stator trailing edge illustrates wide differences between Methods 1 and 5.

The axial velocity for the model stage in ultimate steady flow ($C_{x_{0R}} = C_{x_{0S}} = C_{x_R} = C_{x_S}$) is shown in Fig. 17, and suggests a reversal of flow at the root. Once again the comparison is made with the radial equilibrium solutions for the single stage.

Although the differences between the various theories will be greater because of the low hub-tip ratio chosen, the flow parameter U_t/C_{x_1} is small judged by modern compressor practice, and this small value tends to minimize these differences. This is illustrated in Fig. 18, which compares Methods 1 and 2 for the rotor, at $U_t/C_{x_1} = 1.83$ and 3.0 .

The results of these calculations are summarized in Table I which shows the difference in axial velocity from root to tip, as calculated by various methods for positions 02, 04 and 4.

If Method 5 is considered to be that giving the most accurate calculations, then it is seen from the table that while other methods may give agreement at one trailing-edge position, the results for the other trailing edge are not accurate.

TABLE 1
Differences in C_x root to tip

Method	$\frac{(C_{x02})_{tip} - (C_{x02})_{root}}{C_{x1}}$	$\frac{(C_{x04})_{tip} - (C_{x04})_{root}}{C_{x1}}$	$\frac{(C_{x4})_{tip} - (C_{x4})_{root}}{C_{x1}}$
1. Radial equilibrium	0.47	1.05	1.05
2. Widely spaced discs at blade trailing edges	0.27	0.80	1.07
3. Widely spaced discs at blade centres of pressure	$0.35 \left(\frac{l}{b} 4.2 \right)$	$0.87 \left(\frac{l}{b} 4.2 \right)$	1.01
	$0.40 \left(\frac{l}{b} 2.1 \right)$	$0.87 \left(\frac{l}{b} 2.1 \right)$	0.97
4. Discs at trailing edges. Interference theory (Hawthorne)	$0.40 \left(\frac{l}{b} 4.2 \right)$	0.66	1.04
	$0.32 \left(\frac{l}{b} 2.1 \right)$	0.75	1.09
5. Discs at centres of pressure. Interference theory (Hawthorne)	$0.45 \left(\frac{l}{b} 4.2 \right)$	0.63	0.82
	$0.50 \left(\frac{l}{b} 2.1 \right)$	0.82	0.93
6. Ultimate steady flow	2.0	2.0	
7.			

4. *Conclusions.*—The comparisons of the actuator-disc theories suggest that the choice of the position of the plane of the actuator disc is important, and that methods in which the discs are placed at the trailing edge of the blades may not be as accurate as the original radial equilibrium theory.

For large aspect ratios ($l/b > 3$) the trailing-edge-disc methods may be more satisfactory, but then the effects of blade interference are considerable unless the axial clearances are large compared with the blade width, a configuration not encountered in modern turbo-machines.

For low aspect ratios ($l/b < 3$) blade interference effects become less important, but the placing of the disc at the trailing edge becomes a larger approximation.

The excellent agreement between the theories for blade interference suggest that the use of the attenuation constants k_i , as determined from isolated-disc theory, is justified in a theory taking into account blade interference. It is therefore suggested that Method 5 is of practical use for axial-flow compressor and turbine designers. The disc is placed at the centre of pressure of the blades, but the possibly considerable effects of blade interference are not neglected. The values of k_i are determined directly from the hub-tip ratio.

In turbo-machine design, Method 5 would be used for the first few stages, after which the flow would be expected to approximate to the ultimate steady flow condition soluble by Method 7. Equation (8) may be readily adapted to give the axial velocities at the blade leading edges for determination of the incidences.

A further modification of these methods for the off-design condition may be to allow for variation in outlet air angle and blade losses in the equating of $dH/d\psi$ across the disc, using cascade results and the incidences obtained from the first approximation to obtain values of these two new variables.

It is important to note that Methods 5 and 7, while taking into account any non-uniformity in entry axial velocity profile give no estimation of the growth of the boundary layer through a compressor.

NOTATION

Referring to Figs. 1, 2 and 3, the following notation is used:

Co-ordinates: r, θ, x .

C_r	Radial velocity
C_u	Tangential velocity
C_x	Axial velocity
θ	$= rC_u$ Tangential momentum
η	$= (\partial C_r / \partial x) - (\partial C_x / \partial r)$ Tangential vorticity
ψ	Streamline function defined by: $rC_r = \partial \psi / \partial x \quad rC_x = -(\partial \psi / \partial r)$
H	Stagnation enthalpy
r_t	Tip radius
r_h	Root radius
R	$= r/r_t$ Non-dimensional radius ratio
Ω	Rotor angular velocity
U	$= \Omega r$ Blade speed
α	Absolute air angles
β	Exit rotor air angle measured relative to the moving blade
l	Blade length in radial direction
b	Blade width in axial direction
a	Axial distance between planes of blade trailing edge and centre of pressure

Subscripts:

1	Conditions far upstream of a rotor
2	Conditions far downstream of a rotor
3	Conditions far upstream of a stator
4	Conditions far downstream of a stator
01	Conditions immediately upstream of a rotating actuator disc
02	Conditions immediately downstream of a rotating actuator disc
03	Conditions immediately upstream of a stationary actuator disc
04	Conditions immediately downstream of a stationary actuator disc
2e	Conditions at the trailing edge of a rotor-blade row
4e	Conditions at the trailing edge of a stator-blade row
R	Conditions far downstream of a rotating actuator disc in ultimate steady flow
S	Conditions far downstream of a stationary actuator disc in ultimate steady flow
0R	Conditions at a rotating actuator disc in ultimate steady flow
0S	Conditions at a stationary actuator disc in ultimate steady flow
Re	Conditions at the trailing edge of a rotating blade row in ultimate steady flow
Se	Conditions at the trailing edge of a stationary blade row in ultimate steady flow
t	Relating to blade tip
h	Relating to blade root

Superscripts:

' Denotes perturbation to the axial velocities at infinity (upstream or downstream) in the neighbourhood of an actuator disc, e.g., c_{x1}' , c_{x2}' .

REFERENCES

<i>No.</i>	<i>Author</i>	<i>Title, etc.</i>
1	H. Cohen and E. M. White ..	The theoretical determination of the three-dimensional flow in an axial compressor with special reference to constant reaction blading. A.R.C. 6842. July, 1943.
2	W. Merchant, J. T. Hansford and P. M. Harrison.	The flow of an ideal fluid in an annulus. (Unpublished.) March, 1946.
3	S. L. Bragg and W. R. Hawthorne.	Some exact solutions of the flow through annular cascade actuator discs. <i>J. Ae. Sci.</i> Vol. 17. No. 4. April, 1950.
4	F. E. Marble	The flow of a perfect fluid through an axial-flow turbo-machine with pre-described blade loading. <i>J. Ae. Sci.</i> Vol. 15. No. 8. August, 1948.
5	W. R. Hawthorne	(Unpublished.) 1949.
6	J. W. Raily	The flow of an incompressible fluid through an axial turbo-machine with any number of rows. <i>Aero. Quart.</i> Vol. III. September, 1951.
7	A. R. Howell	(Unpublished.) 1942.
8	F. Ruden	Investigation of single-stage axial-flow fans. N.A.C.A. T.M. 1062.
9	Jahnke and Emde	<i>Tables of Functions.</i> Dover Publications. 1945.

APPENDIX I

Three-Dimensional Flow in an Axial Turbo-Machine

1. *The Approximate Solution for Flow through an Actuator Disc.*—An approximate solution of the actuator-disc problem may be obtained by assuming that the trailing vortex lines lie on cylindrical surfaces concentric with the axis of the annulus. The radial velocities are not, however, neglected, so that the condition for stream surfaces and vortex-line surfaces to be the same is no longer satisfied.

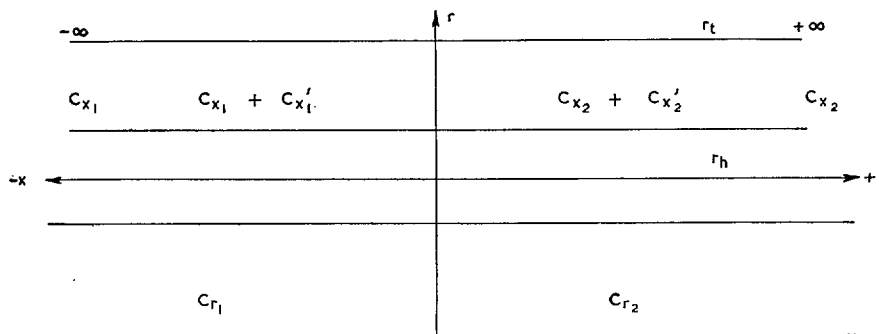


FIG. A.1.

With this assumption it may be shown (Ref. 8) that the axial velocity at the actuator disc is $(C_{x_1} + C_{x_2})/2$ where C_{x_1} and C_{x_2} are the axial velocities at infinity upstream and downstream respectively. With the notation of the figure C_{x_1}' and C_{x_2}' are the perturbations to the axial velocities in the regions $x = 0$ to $x = -\infty$ and $x = 0$ to $x = +\infty$ respectively. At $x = 0$ $C_{x_1}' = (C_{x_2} - C_{x_1})/2$ and $C_{x_2}' = (C_{x_1} - C_{x_2})/2$.

Since it is assumed that the ring vortices pass downstream along cylindrical surfaces the value of the tangential vorticity, η , at any radius will be constant and is equal to its value at infinity.

Vorticity components in a flow with velocities C_r, C_u, C_x and co-ordinates r, θ, x , are ξ, η, ζ , where for axially symmetric flow:

$$\left. \begin{aligned} \xi &= -\frac{\partial C_u}{\partial x} \\ \eta &= \frac{\partial C_r}{\partial x} - \frac{\partial C_x}{\partial r} \end{aligned} \right\} \zeta = \frac{1}{r} \frac{\partial}{\partial r} (r C_u) \quad \dots \dots \dots (1)$$

For incompressible, axially symmetric, flow the continuity equation is

$$\frac{\partial}{\partial x} (r C_x) + \frac{\partial}{\partial r} (r C_r) = 0 \quad \dots \dots \dots (2)$$

Hence
$$\eta = \frac{\partial C_r}{\partial x} - \frac{\partial}{\partial r} (C_x r + \partial C_x r') = -\frac{\partial C_x r}{\partial r} \quad \dots \dots \dots (3)$$

or
$$\frac{\partial C_r}{\partial x} = \frac{\partial C_x r'}{\partial r}$$

A similar equation applies upstream of the actuator disc. The equation of continuity (2) for incompressible flow may be written:

$$\frac{\partial C_x r'}{\partial x} + \frac{1}{r} \frac{\partial}{\partial r} (r C_r) = 0 \quad \dots \dots \dots (4)$$

Differentiating equation (4) partially with respect to r and substituting from equation (3):

$$\frac{\partial^2 C_r}{\partial r^2} + \frac{1}{r} \frac{\partial C_r}{\partial r} - \frac{C_r}{r^2} + \frac{\partial^2 C_x r}{\partial x^2} = 0 \quad \dots \dots \dots (5)$$

A standard procedure for solving this equation is to write $C_r = \sum_{i=1}^{i=\infty} \{\exp(k_i x)\} f_i(r)$, where k_i with $i = 1, 2, 3$, etc., are a number of constants whose values depend on the boundary conditions. Then:

$$\sum_i \{\exp(k_i x)\} f_i''(r) + \frac{1}{r} \sum_i \{\exp(k_i x)\} f_i'(r) + \sum_i \left(k_i^2 - \frac{1}{r^2}\right) \{\exp(k_i x)\} f_i(r) = 0 \quad \dots \dots (6)$$

Hence for all values of i since this equation must be satisfied at all r and $x > 0$ or $x < 0$,

$$f_i''(r) + \frac{1}{r} f_i'(r) + \left(k_i^2 - \frac{1}{r^2}\right) f_i(r) = 0 \quad \dots \dots \dots (7)$$

The general solution of this Bessel's differential equation is:

$$f_i(r) = A_i J_1(k_i r) + B_i Y_1(k_i r) \quad \dots \dots \dots (8)$$

Hence the radial velocity is given by:

$$C_r = \sum_i \{\exp(k_i x)\} \{A_i J_1(k_i r) + B_i Y_1(k_i r)\} \quad \dots \dots \dots (9)$$

Since at the boundaries of the annulus $r = r_h$ and $r = r_i$, $C_r = 0$.

$$A_i J_1(k_i r_i) + B_i Y_1(k_i r_i) = 0$$

and

$$A_i J_1(k_i r_h) + B_i Y_1(k_i r_h) = 0$$

or

$$J_1(k_i r_h) Y_1(k_i r_i) - J_1(k_i r_i) Y_1(k_i r_h) = 0 \quad \dots \dots \dots (10)$$

This equation gives an infinite number of values of k_i ; the first six of which are tabulated for various values of (r_i/r_h) by Janke and Emde (p. 205).

Since the values of k_i only depend on the values of r_i and r_h , the solutions for C_{r_1} and C_{r_2} are symmetrical about the actuator disc.

Substituting for C_r in equation (4) and integrating to obtain C_x' between the limits $x = 0$ and $x = \pm \infty$:

$$\sum_i [\{\exp(k_i x)\}/k_i] \left[f_i'(r) + \frac{1}{r} f_i(r) \right] = C_x' \quad \dots \quad \dots \quad \dots \quad \dots \quad (11)$$

Now since C_r and $C_x' = 0$ at $x = \pm \infty$, k_i is negative for $x > 0$ and positive for $x < 0$.

Inserting the values for C_x' at $x = 0$:

$$\sum_i \frac{1}{k_i} \left[f_i'(r) + \frac{1}{r} f_i(r) \right] = \frac{C_{x_2} - C_{x_1}}{2} \quad \dots \quad \dots \quad \dots \quad \dots \quad (12)$$

If only the first root of equation (11) is taken, then:

$$C_{x_1}' = (\exp kx) \left(\frac{C_{x_2} - C_{x_1}}{2} \right), \quad \dots \quad \dots \quad \dots \quad \dots \quad \dots \quad (13a)$$

$$C_{x_2}' = - \{ \exp(-kx) \} \left(\frac{C_{x_2} - C_{x_1}}{2} \right) \quad \dots \quad \dots \quad \dots \quad \dots \quad \dots \quad (13b)$$

Hence if l is the blade length:

$$C_{x_1}' = - C_{x_2}' = \left(\exp \frac{3 \cdot 16x}{l} \right) \left(\frac{C_{x_2} - C_{x_1}}{2} \right) \quad \dots \quad \dots \quad \dots \quad \dots \quad (14)$$

The value of 3.16 is correct for $r_i/r_h = 1.5$ and varies between 3.146 and 3.23 as r_i/r_h varies from 1.2 to 2.5 respectively.

2. *Blade-Interference Theory.*—Between each blade row in the compressor, sheets of tangential smoke-ring vortices exist which are identified by the value of C_x at downstream infinity. These are shown diagrammatically in Fig. 2.

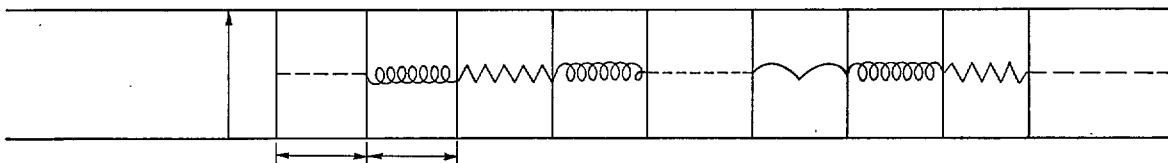


FIG. A.2. Diagrammatic representation of sheets of tangential vorticity between blade rows.

If the p th row of blades shown in Fig. A.3 is considered and all the vortex sheets of neighbouring blades are superimposed:

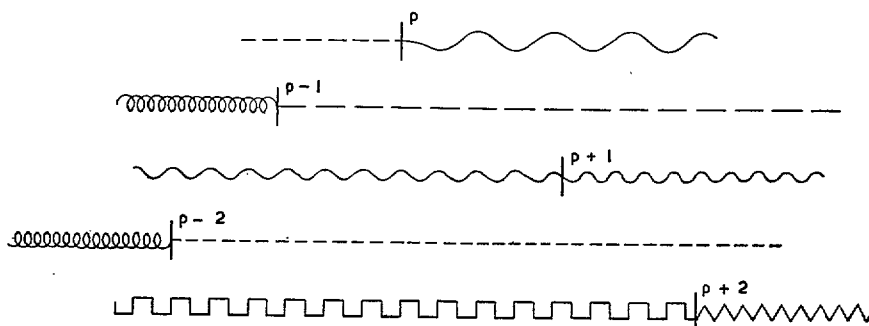


FIG. A.3.

The sum of all these vortex sheets is pictured below where the compressor has n stages:

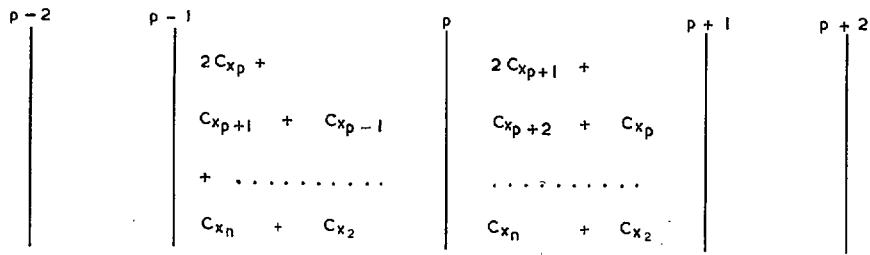


FIG. A.4.

Hence between the $(p - 1)$ th and the p th rows the vortex sheets obtained by superposition are:

$$C_{x_p} + \sum_{q=2}^{q=n} C_{x_q} .$$

Downstream of the p th row and ahead of the $(p + 1)$ th the vortex sheets sum to:

$$C_{x_{p+1}} + \sum_{q=2}^{q=n} C_{x_q} .$$

Hence the vorticity pattern may be obtained by summing the vorticities of all rows taken separately and subtracting the sum of all the vortex sheets due to each blade stretching from upstream to downstream infinity. This procedure is shown diagrammatically in Fig. A.5 for a single stage:

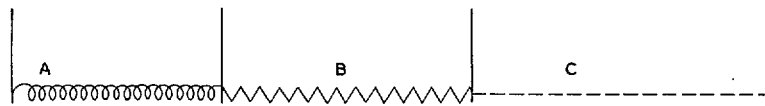


FIG. A.5a. Actual vorticity.

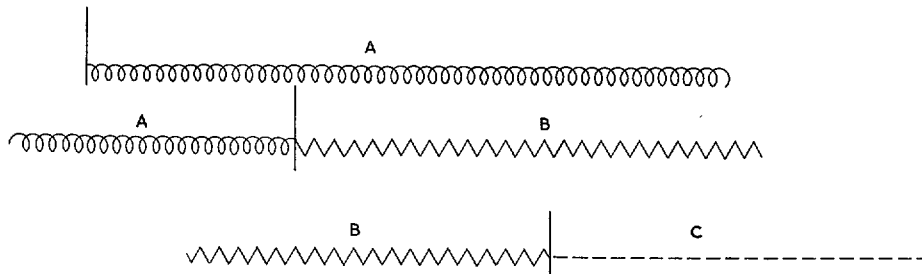


FIG. A.5b. Each row taken separately.

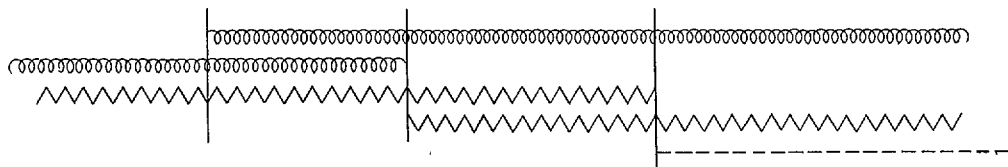


FIG. A.5c. Sum of vorticities due to each row taken separately.

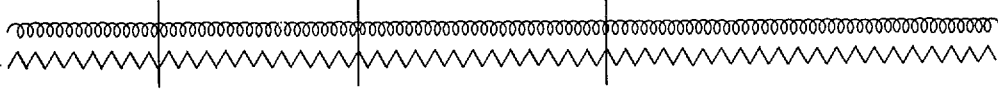


FIG. A.5d. Vortex sheets extending to infinity which require to be subtracted from (c) to give (a).

The induced axial velocity at the p th row due to the q th row when the vortices of all rows are taken separately is from equation (14),

When $q < p$:

$$\begin{aligned}
 &= C_{xq+1} - \left\{ \exp \left(-\frac{k_q}{l_q} x_{pq} \right) \right\} \left(\frac{C_{xq+1} - C_{xq}}{2} \right) - C_{x1q} \\
 &= \frac{(C_{xq+1} + C_{xq})}{2} + \frac{(C_{xq+1} - C_{xq})}{2} \left(1 - \left\{ \exp \left(-\frac{k_q}{l_q} x_{pq} \right) \right\} \right) - C_{x1q} \dots \dots \quad (15)
 \end{aligned}$$

When $q > p$:

$$\begin{aligned}
 &= C_{xq} + \left\{ \exp \left(-\frac{k_q}{l_q} x_{pq} \right) \right\} \left(\frac{C_{xq+1} - C_{xq}}{2} \right) - C_{x1q} \\
 &= \left(\frac{C_{xq+1} + C_{xq}}{2} \right) - \left(\frac{C_{xq+1} - C_{xq}}{2} \right) \left(1 - \left\{ \exp \left(-\frac{k_q}{l_q} x_{pq} \right) \right\} \right) - C_{x1q}, \quad \dots \quad (16)
 \end{aligned}$$

where x_{pq} is the magnitude (always positive) of the axial distance between p th and q th rows and C_{x1q} is the average axial velocity at the q th row:

$$C_{x1q} = \frac{W}{\rho_m \pi (r_i^2 - r_h^2)} \dots \dots \dots \quad (17)$$

From the sum of the above induced velocities must be subtracted the effect of all the infinitely long vortices due to each blade row as shown in Fig. A.5. This latter effect is:

$$\sum_{q=2}^{q=n} (C_{xq} - C_{x1q}) \dots \dots \dots \quad (18)$$

Hence, the total induced velocity is:

$$\begin{aligned}
 &\sum_{q=1}^{q=n} \left\{ \left(\frac{C_{xq+1} + C_{xq}}{2} \right) \pm \left(\frac{C_{xq+1} - C_{xq}}{2} \right) \left(1 - \left\{ \exp \left(-\frac{k_q}{l_q} x_{pq} \right) \right\} \right) - C_{x1q} \right\} \\
 &\quad - \sum_{q=2}^{q=n} (C_{xq} - C_{x1q}), \quad \dots \dots \dots \quad (19)
 \end{aligned}$$

noting that the + sign is taken when $q < p$ and the - sign when $q > p$. The induced velocity may also be written:

$$\begin{aligned}
 &\sum_{q=1}^{q=p-1} - \left(\frac{C_{xq+1} - C_{xq}}{2} \right) \left\{ \exp \left(-\frac{k_q}{l_q} x_{pq} \right) \right\} + \left(\frac{C_{xp+1} + C_{xp}}{2} \right) \\
 &\quad + \sum_{p+1}^n \left(\frac{C_{xq+1} - C_{xq}}{2} \right) \left\{ \exp \left(-\frac{k_q}{l_q} x_{pq} \right) \right\} - C_{x1} \dots \dots \dots \quad (20)
 \end{aligned}$$

Hence the axial velocity at the p th row is :

$$\begin{aligned}
 C_{x0p} = & \left(\frac{C_{xp+1} + C_{xp}}{2} \right) + (C_{x1p} - C_{x1}) \\
 & - \sum_{q=1}^{q=p-1} \left(\frac{C_{xq+1} - C_{xq}}{2} \right) \left\{ \exp \left(- \frac{k_q}{l_q} x_{pq} \right) \right\} \\
 & + \sum_{q=p+1}^{q=n} \left(\frac{C_{xq+1} - C_{xq}}{2} \right) \left\{ \exp \left(- \frac{k_q}{l_q} x_{pq} \right) \right\} \quad \dots \quad \dots \quad \dots \quad \dots \quad (21)
 \end{aligned}$$

or for incompressible flow :

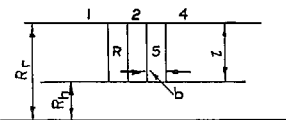
$$\begin{aligned}
 C_{x0p} = & \left(\frac{C_{xp+1} + C_{xp}}{2} \right) - \sum_{q=1}^{q=p-1} \left(\frac{C_{xq+1} - C_{xq}}{2} \right) \left\{ \exp \left(- \frac{k_q}{l_q} x_{pq} \right) \right\} \\
 & + \sum_{q=p+1}^{q=n} \left(\frac{C_{xq+1} - C_{xq}}{2} \right) \left\{ \exp \left(- \frac{k_q}{l_q} x_{pq} \right) \right\} \quad \dots \quad \dots \quad \dots \quad \dots \quad (22)
 \end{aligned}$$

Similarly it may be shown that the axial velocity at a point x_{pe} between the p th and $(p + 1)$ th rows is given by :

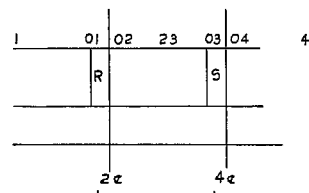
$$\begin{aligned}
 C_{xpe} = & C_{xp+1} - \sum_{q=1}^{q=p} \left(\frac{C_{xq+1} - C_{xq}}{2} \right) \left\{ \exp \left(- \frac{k_q}{l_q} x_{peq} \right) \right\} \\
 & + \sum_{q=p+1}^{q=n} \left(\frac{C_{xq+1} - C_{xq}}{2} \right) \left\{ \exp \left(- \frac{k_q}{l_q} x_{peq} \right) \right\} \quad \dots \quad \dots \quad \dots \quad \dots \quad (23)
 \end{aligned}$$

where x_{peq} is the distance (always positive) between the plane $x = x_{pe}$ and the q th disc.

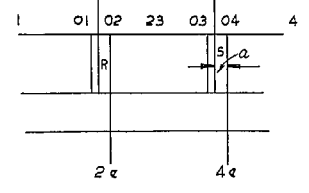
23



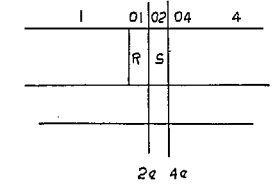
Method 1.
 Radial equilibrium at trailing edges of blades.



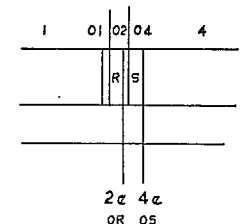
Method 2.
 Widely spaced actuator discs at trailing edges of blades.



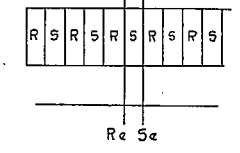
Method 3.
 Widely spaced actuator discs at centres of pressure of blades.
 $(\frac{l}{b} = 2.1, 4.2 \quad \frac{a}{b} = \frac{2}{3})$



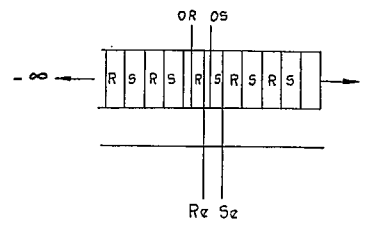
Method 4.
 Blade interference discs at trailing edges of blades
 $(\frac{l}{b} = 2.1, 4.2)$



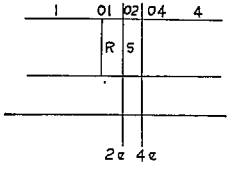
Method 5.
 Blade interference. Discs at centres of pressure of blades.
 $\frac{l}{b} = 2.1, 4.2 \quad \frac{a}{b} = \frac{2}{3}$



Method 6.
 Ultimate steady flow. Discs at trailing edges of blades.
 $(\frac{l}{b} = 2.1, 4.2)$



Method 7.
 Ultimate steady flow. Discs at centres of pressure of blades.
 $(\frac{l}{b} = 2.1, 4.2 \quad \frac{a}{b} = \frac{2}{3})$



Method 8.
 Rully's method. Discs at trailing edges of blades.

FIGS. 1 and 2. Methods used in calculation of flow through model stage.

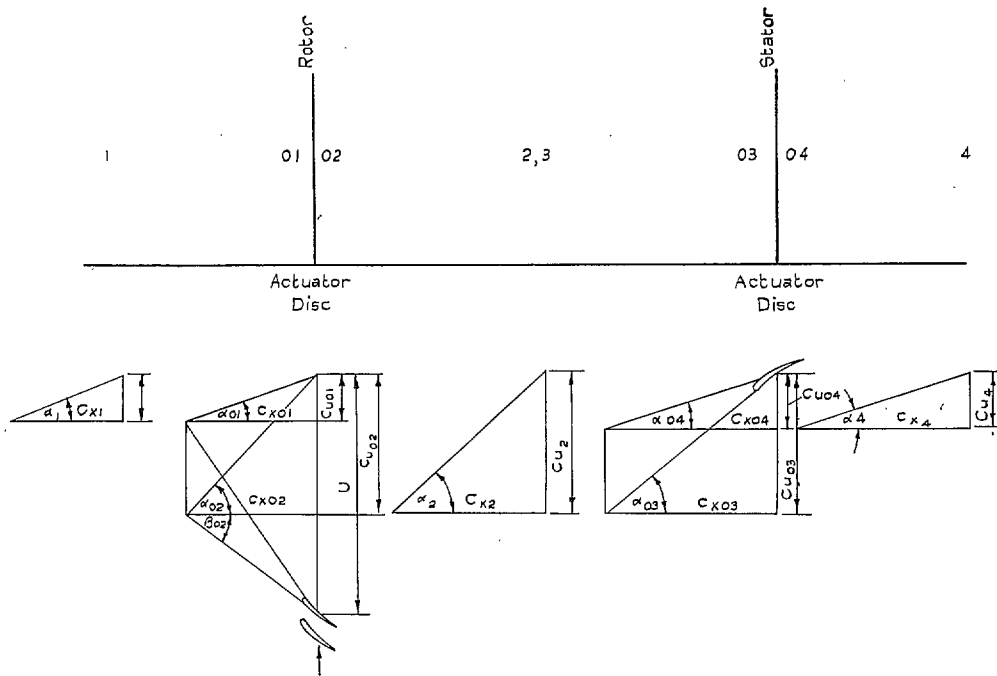


FIG. 3. Model-stage velocity triangles.

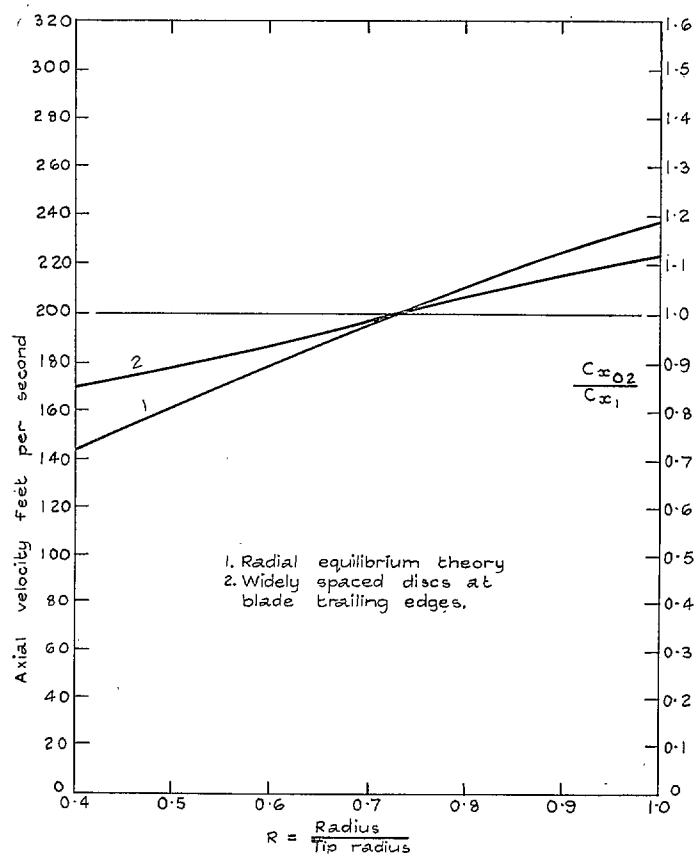


FIG. 4. Model stage—Axial velocity at rotor trailing edge.

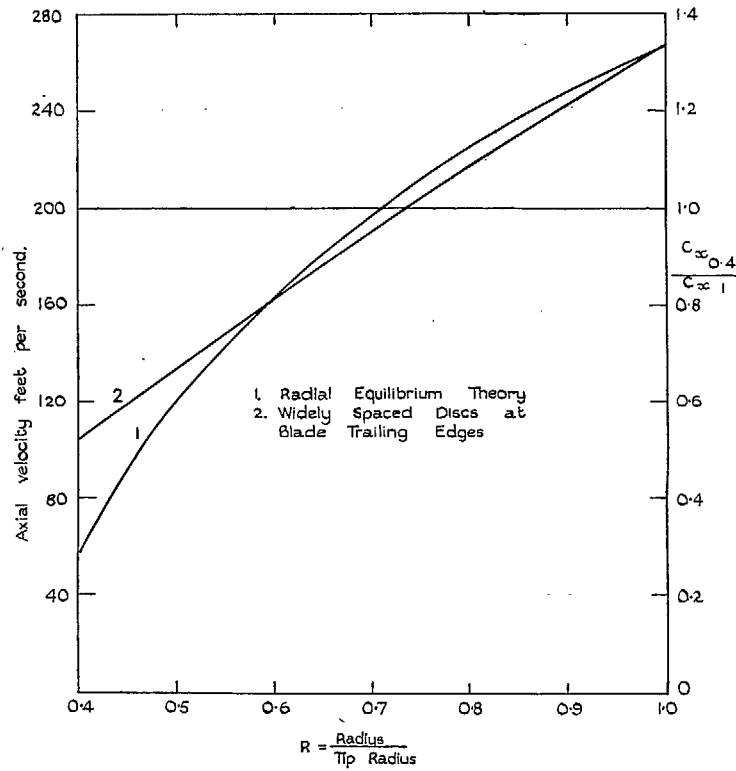


FIG. 5. Model stage—Axial velocity at stator trailing edge.

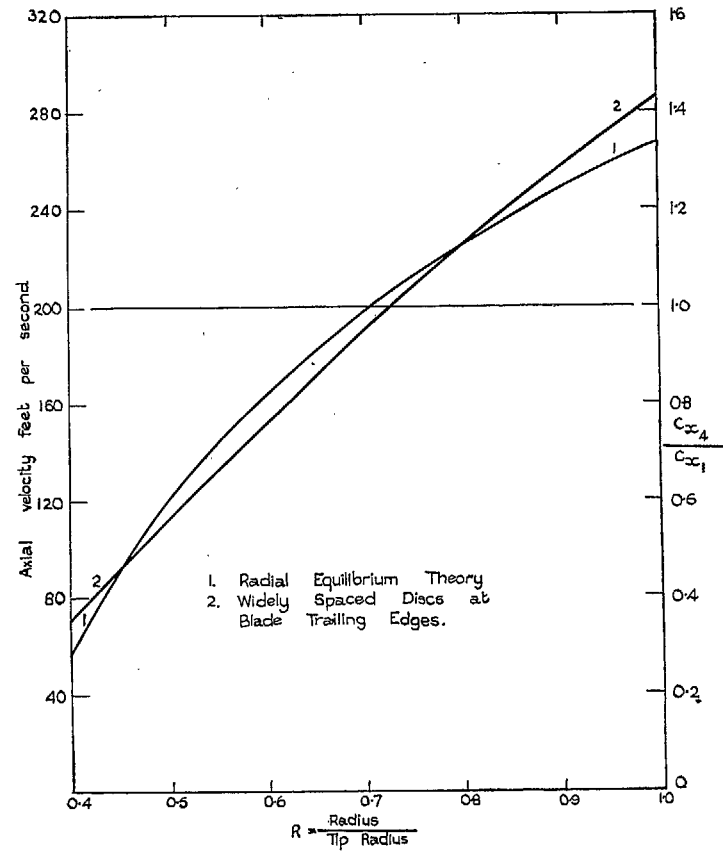


FIG. 6. Model stage—Axial velocity far downstream of stator.

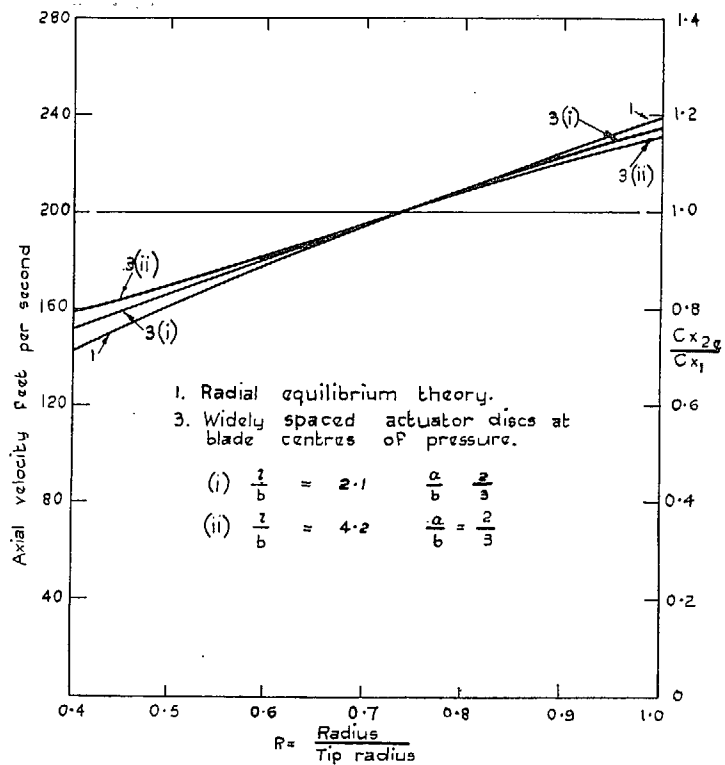


FIG. 7. Model stage—Axial velocity at rotor trailing edge.

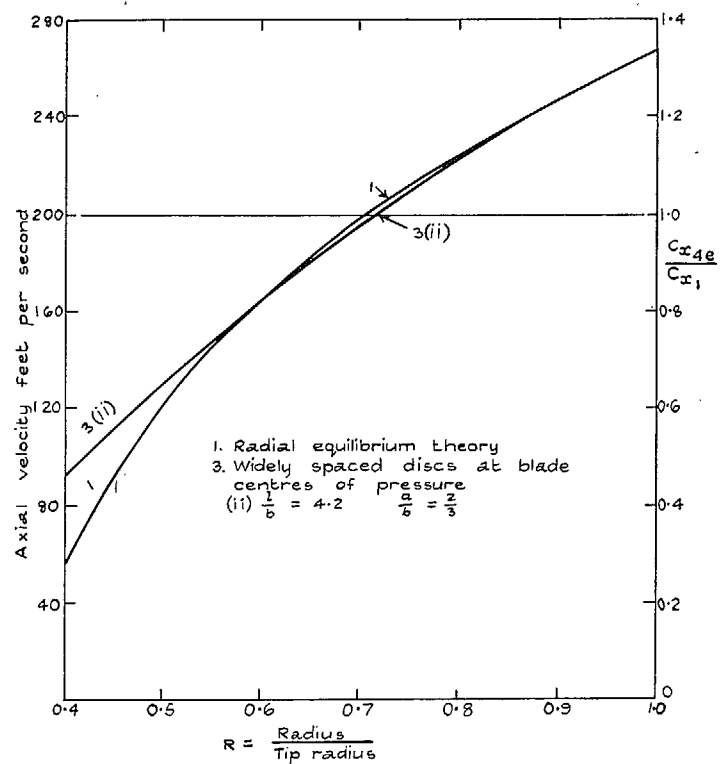


FIG. 8. Model stage—Axial velocity at stator trailing edge.

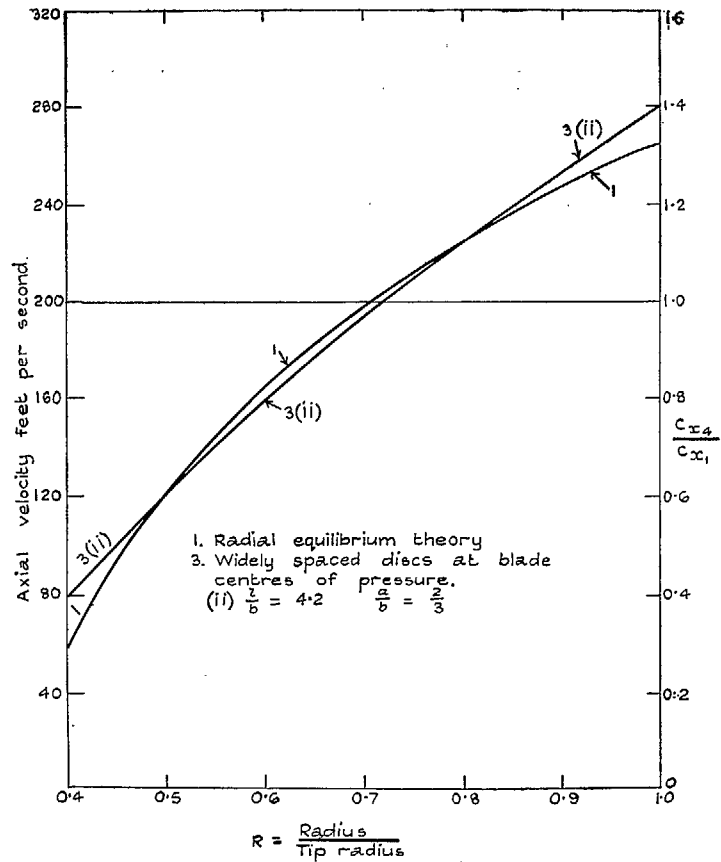


FIG. 9. Model stage—Axial velocity far downstream of stator.

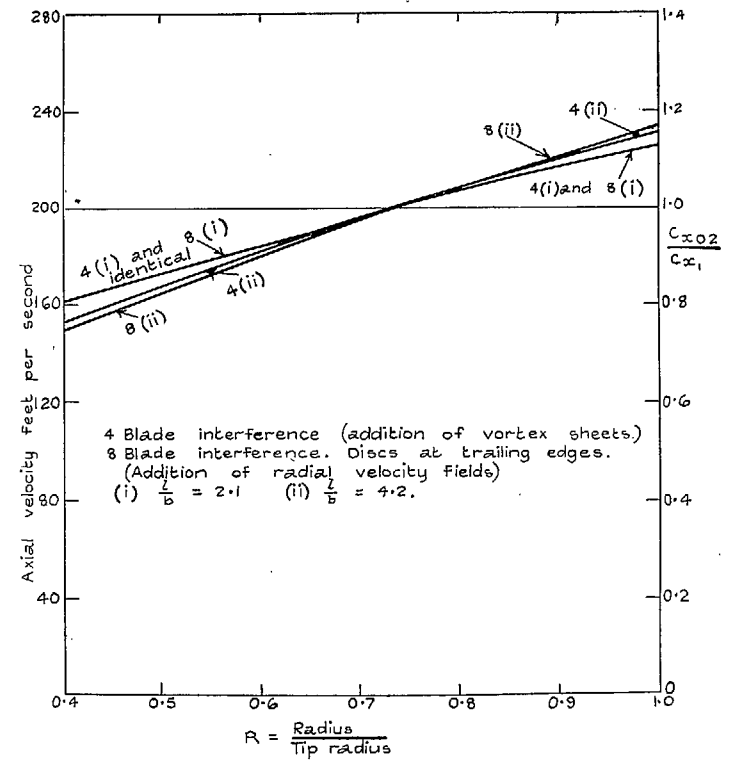


FIG. 10. Model stage—Axial velocity at rotor trailing edges.

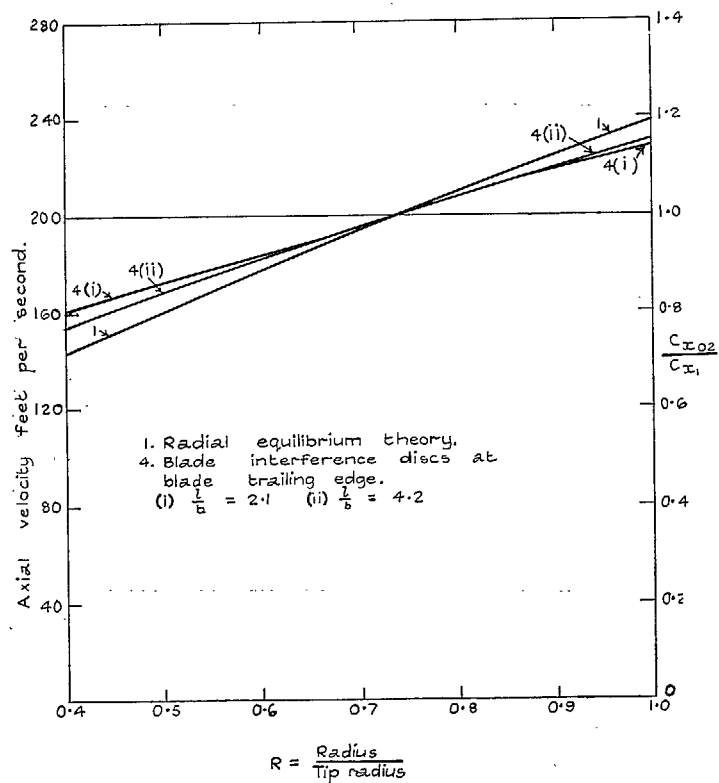


FIG. 11. Model stage—Axial velocity at rotor trailing edge.

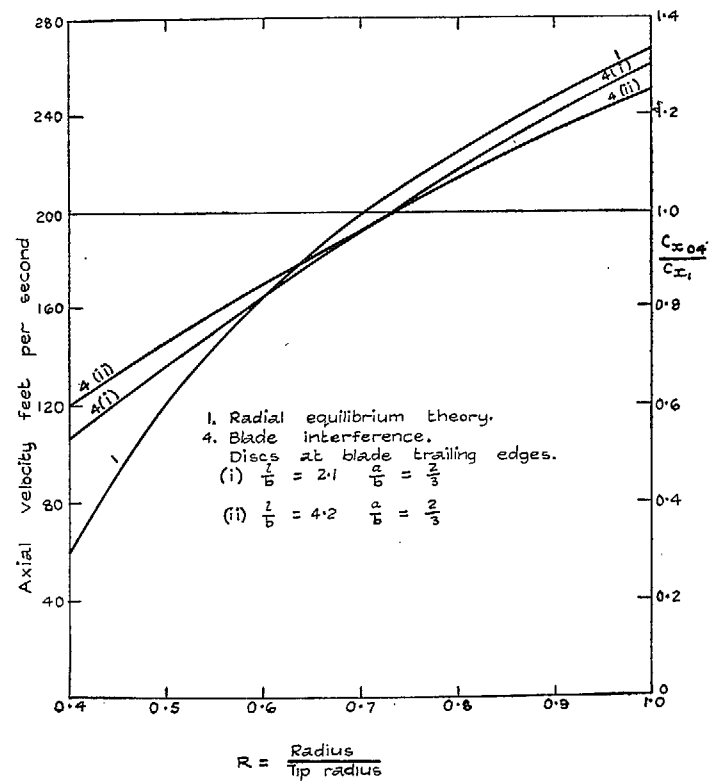


FIG. 12. Model stage—Axial velocities at stator trailing edge.

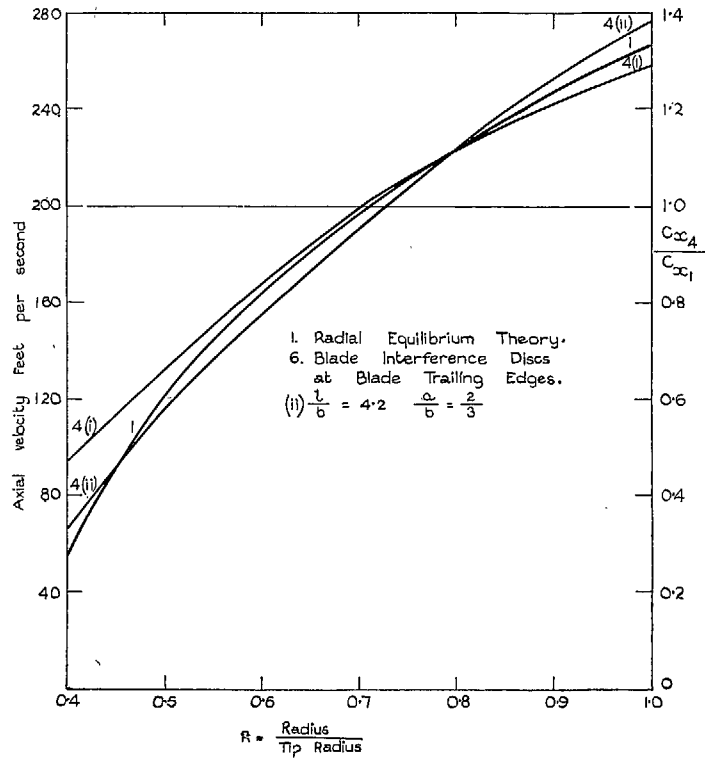


FIG. 13. Model stage—Axial velocities far downstream of stator.

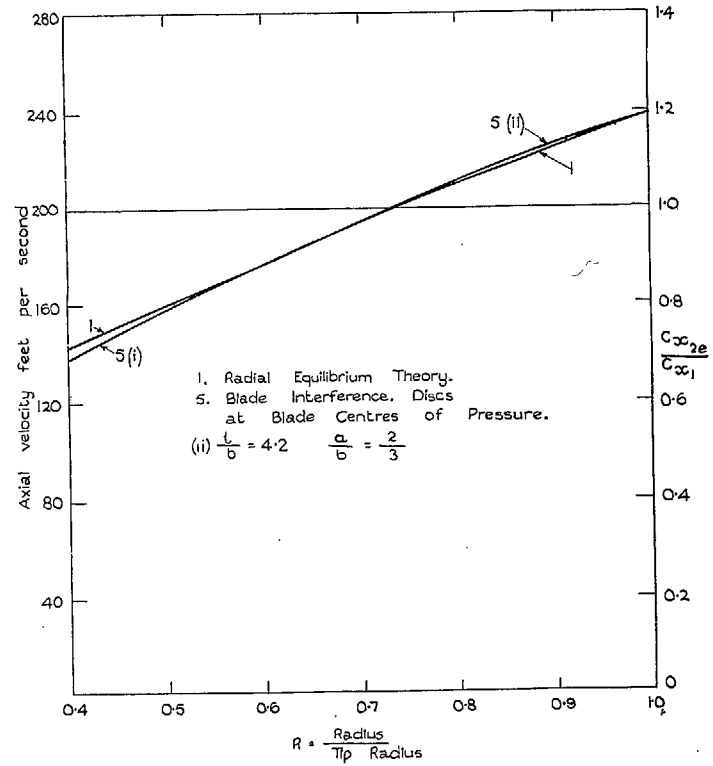


FIG. 14. Model stage—Axial velocity at rotor trailing edge.

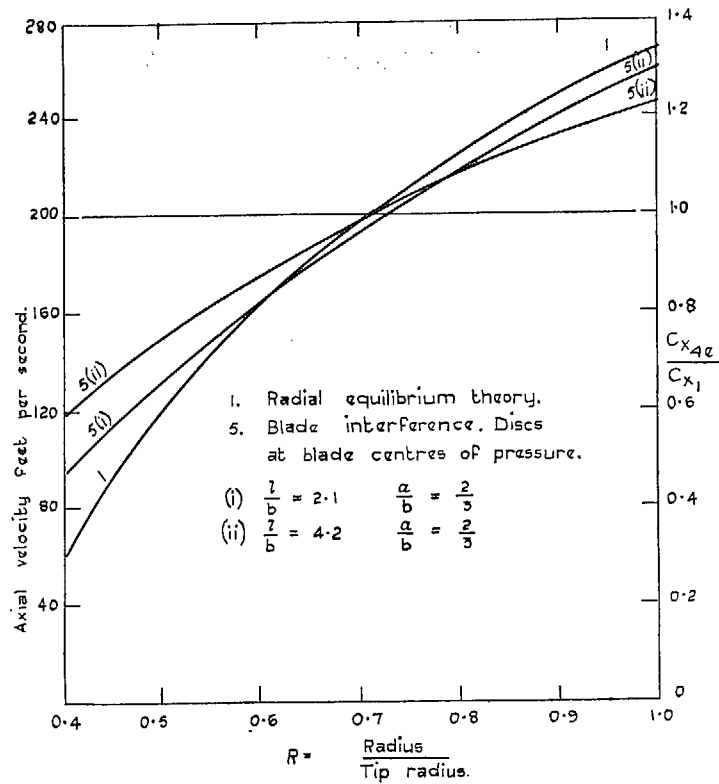


FIG. 15. Model stage—Axial velocity at stator trailing edges.

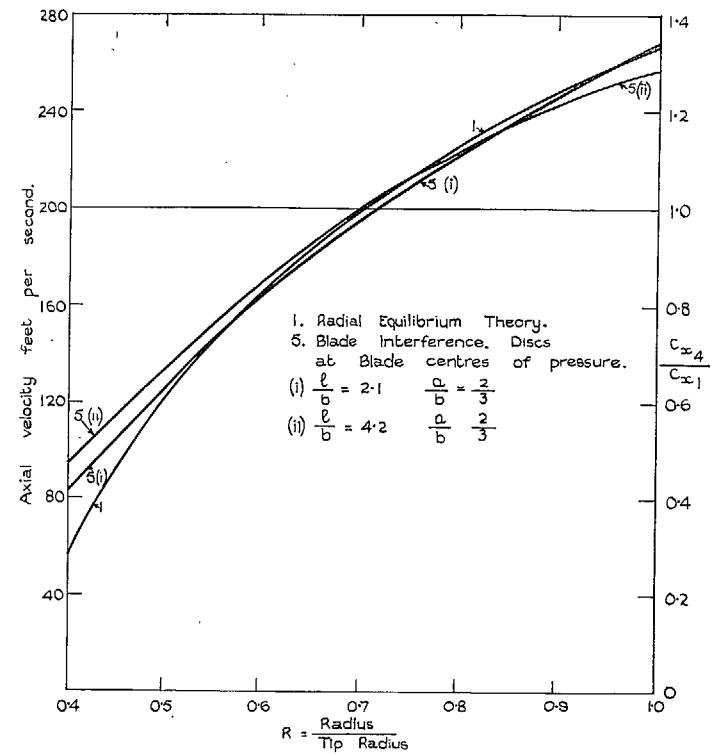


FIG. 16. Model stage—Axial velocities far downstream of stator.

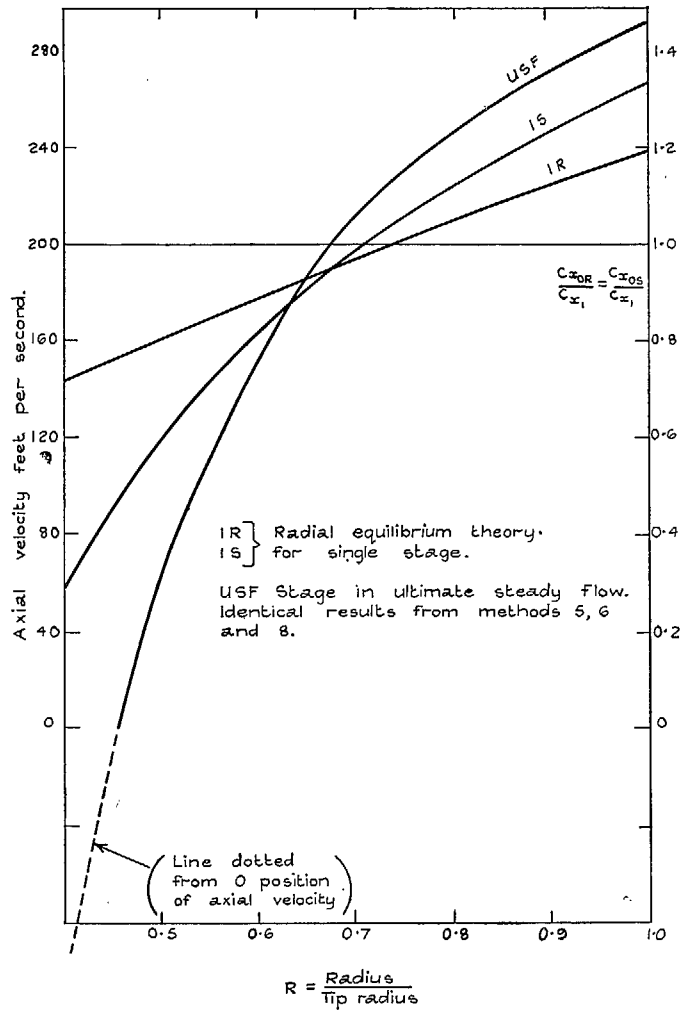


FIG. 17. Model stage—Axial velocities in ultimate steady flow.

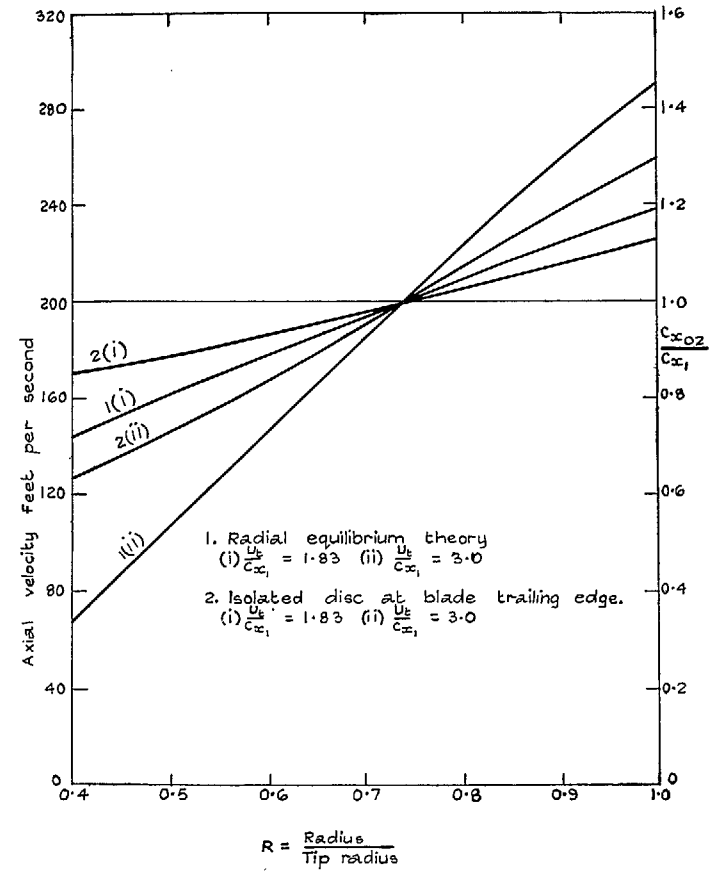


FIG. 18. Model stage—Axial velocity at rotor trailing edge.

Publications of the Aeronautical Research Council

ANNUAL TECHNICAL REPORTS OF THE AERONAUTICAL RESEARCH COUNCIL (BOUND VOLUMES)

- 1939 Vol. I. Aerodynamics General, Performance, Airscrews, Engines. 50s. (52s.).
 Vol. II. Stability and Control, Flutter and Vibration, Instruments, Structures, Seaplanes, etc.
 63s. (65s.)
- 1940 Aero and Hydrodynamics, Aerofoils, Airscrews, Engines, Flutter, Icing, Stability and Control,
 Structures, and a miscellaneous section. 50s. (52s.)
- 1941 Aero and Hydrodynamics, Aerofoils, Airscrews, Engines, Flutter, Stability and Control,
 Structures. 63s. (65s.)
- 1942 Vol. I. Aero and Hydrodynamics, Aerofoils, Airscrews, Engines. 75s. (77s.).
 Vol. II. Noise, Parachutes, Stability and Control, Structures, Vibration, Wind Tunnels.
 47s. 6d. (49s. 6d.)
- 1943 Vol. I. Aerodynamics, Aerofoils, Airscrews. 80s. (82s.)
 Vol. II. Engines, Flutter, Materials, Parachutes, Performance, Stability and Control, Structures.
 90s. (92s. 9d.)
- 1944 Vol. I. Aero and Hydrodynamics, Aerofoils, Aircraft, Airscrews, Controls. 84s. (86s. 6d.)
 Vol. II. Flutter and Vibration, Materials, Miscellaneous, Navigation, Parachutes, Performance,
 Plates and Panels, Stability, Structures, Test Equipment, Wind Tunnels.
 84s. (86s. 6d.)
- 1945 Vol. I. Aero and Hydrodynamics, Aerofoils. 130s. (132s. 9d.)
 Vol. II. Aircraft, Airscrews, Controls. 130s. (132s. 9d.)
 Vol. III. Flutter and Vibration, Instruments, Miscellaneous, Parachutes, Plates and Panels,
 Propulsion. 130s. (132s. 6d.)
 Vol. IV. Stability, Structures, Wind Tunnels, Wind Tunnel Technique. 130s. (132s. 6d.)

Annual Reports of the Aeronautical Research Council—

1937 2s. (2s. 2d.) 1938 1s. 6d. (1s. 8d.) 1939-48 3s. (3s. 5d.)

Index to all Reports and Memoranda published in the Annual Technical Reports, and separately—

April, 1950 - - - R. & M. 2600 2s. 6d. (2s. 10d.)

Author Index to all Reports and Memoranda of the Aeronautical Research Council—

1909—January, 1954 R. & M. No. 2570 15s. (15s. 8d.)

Indexes to the Technical Reports of the Aeronautical Research Council—

December 1, 1936—June 30, 1939	R. & M. No. 1850	15s. 3d. (15s. 5d.)
July 1, 1939—June 30, 1945	R. & M. No. 1950	15s. (15s. 2d.)
July 1, 1945—June 30, 1946	R. & M. No. 2050	15s. (15s. 2d.)
July 1, 1946—December 31, 1946	R. & M. No. 2150	15s. 3d. (15s. 5d.)
January 1, 1947—June 30, 1947	R. & M. No. 2250	15s. 3d. (15s. 5d.)

Published Reports and Memoranda of the Aeronautical Research Council—

Between Nos. 2251-2349	R. & M. No. 2350	15s. 9d. (15s. 11d.)
Between Nos. 2351-2449	R. & M. No. 2450	2s. (2s. 2d.)
Between Nos. 2451-2549	R. & M. No. 2550	2s. 6d. (2s. 10d.)
Between Nos. 2551-2649	R. & M. No. 2650	2s. 6d. (2s. 10d.)
Between Nos. 2651-2749	R. & M. No. 2750	2s. 6d. (2s. 10d.)

Prices in brackets include postage

HER MAJESTY'S STATIONERY OFFICE

York House, Kingsway, London W.C.2; 423 Oxford Street, London W.1; 13a Castle Street, Edinburgh 2;
 39 King Street, Manchester 2; 2 Edmund Street, Birmingham 3; 109 St. Mary Street, Cardiff; Tower Lane, Bristol 1;
 80 Chichester Street, Belfast, or through any bookseller.